Rocznik Ochrona Środowiska

Volume 26 Year 2024 ISSN 2720-7501 pp. 638-657

https://doi.org/10.54740/ros.2024.056 open access

Received: May 2024 Accepted: October 2024 Published: December 2024

Comparative Analysis and Kinetic Modeling of Marbofloxacin Degradation via Electro-Fenton and Biodegradation Optimization

Rabab A. Hakami[1], Muna Shueai Yahya[2], Mohamed El Bakkali[3], Afnan A. Hakami[4]*

[1]Chemistry Department, Faculty of Science, King Khalid University, Abha, Saudi Arabia
https://orcid.org/0009-0002-2703-7658

[2]Department of Chemistry, Faculty of Education, Hodeidah University, Hodeidah, Yemen
https://orcid.org/0009-0003-4316-0223

[3]Department of Biology, Faculty of Sciences, Ibn Tofail University, Morocco,
Higher Institute of Nursing Professions and Health Technologies, Kenitra Annex, Morocco
https://orcid.org/0000-0003-3160-8556

[4]Department of Chemistry, College of Science, Princess Nourah bint Abdulrahman University, Riyadh, Saudi Arabia
https://orcid.org/0000-0002-8936-2432

[*]corresponding author's e-mail: munayahya980@gmail.com

Abstract: In the quest for sustainable water purification methods, electrochemical Advanced Oxidation Processes (AOPs) emerge as pivotal strategies against organic pollutants. This study delves into the efficacy of the Electro-Fenton process, a distinguished AOP that leverages the in-situ generation of hydroxyl radicals (•OH) via the electrochemical reduction of oxygen. By conducting systematic experiments in deionized water, we evaluate the influence of catalyst concentration, applied current density, and cathode material selection on the degradation kinetics of marbofloxacin – a model pharmaceutical pollutant. Employing advanced statistical and kinetic modeling, our investigation reveals critical insights into the process dynamics, uncovering the nuanced interplay between operational parameters and degradation efficiency. The findings substantiate the Electro-Fenton process as an environmentally advantageous and effective solution for water decontamination and advancing the field of water purification technology.

Keywords: Electro-Fenton, AOPs, degradation, Marbofloxacin, HPLC

1. Introduction

Conventional water treatment plants often fall short of addressing contamination effectively. However, advanced oxidation processes (AOPs) distinguish themselves as formidable methods for eliminating diverse organic pollutants from water. At the core of these treatments is the generation of potent oxidants, particularly hydroxyl radicals (•OH), which possess a substantial oxidation-reduction potential of 2.8 V/SHE, ranking just below fluorine in terms of oxidizing strength. Under optimal conditions, these radicals can mineralize completely, breaking down organic contaminants and any by-products formed during oxidation (Sirés et al. 2014, Ganiyu et al. 2021, Arhoutane et al. 2019).

Amongst various AOPs, the Electro-Fenton process distinguishes itself through the homogeneous generation of •OH in solution, a characteristic that arises from its electrochemical foundation. This sets it apart from traditional Fenton reactions, which rely on the external addition of H_2O_2 and iron ions. The in-situ production of H_2O_2 through oxygen reduction is a crucial reaction (Equation 2), and the simultaneous cathodic reduction of Fe^{3+} to Fe^{2+} ions further facilitates this process (Brillas et al. 2009, Nidheesh et al. 2012, Oturan et al. 2018, Zhou et al. 2018).

$$Fe^{2+}+H_2O_2 \rightarrow Fe^{3+}+OH^- + {}^{\bullet}OH \quad (1)$$

$$O_2+2H^++2e^- \rightarrow H_2O_2 \quad (2)$$

$$Fe^{3+}+e^- \rightarrow Fe^{2+} \quad (3)$$

The procedural efficacy hinges on a consistent supply of H_2O_2 to the solution, with cathode material selection playing a pivotal role in the process efficiency (Sopaj et al. 2016). Carbonaceous materials, such as carbon felt (Lahkimi et al. 2007, Zazou et al. 2019), carbon sponge (Özcan et al. 2008), and graphite (Nidheesh et al. 2014), are favored due to their ability to generate H_2O_2, thus enhancing •OH production via Equation 1.

Recognizing the complexity of these electrochemical interactions, this study employs a robust statistical modeling approach to dissect and understand the dynamics governing the degradation kinetics of marbofloxacin. We aim to capture the nuanced interplay between catalyst concentration, applied current density, and cathode material efficacy by developing linear and nonlinear models. These models are not merely academic

exercises but are critical tools that bridge theoretical understanding with practical application. They allow us to predict the outcomes of electrochemical reactions under various conditions and to optimize the parameters for enhanced treatment effectiveness.

Carbonaceous materials are prevalently utilized within the Electro-Fenton framework due to their mechanical and chemical resilience, cost-effectiveness, conductivity, non-toxicity, and porosity.

The objective of this research is twofold: first, to evaluate and compare the efficacy of two cathode materials in terms of their $^{\bullet}OH$ generation rates, and second, to elucidate the influence of catalyst concentration and applied current density on the efficiency of the Electro-Fenton process through advanced statistical modeling. The focal pollutant examined is marbofloxacin, a fluoroquinolone antibiotic widely used in veterinary medicine. Upon release into agricultural wastewater, its degradation, and mineralization have prompted considerable scrutiny (Sturini et al. 2015).

The research was conducted in deionized water to simplify kinetic studies and facilitate identifying and quantifying degradation by-products (Rabab A. Hakami et al. 2024). A comprehensive comparison of performance was made, considering marbofloxacin decay kinetics, time required to complete oxidation, mineralization rate, and Instantaneous Current Efficiency (ICE). The anticipated findings from this study are expected to be instrumental in identifying an optimal cathode for the Electro-Fenton process, thus bolstering the method's overall effectiveness. The determination of the ratio of biochemical oxygen demand (BOD) to chemical oxygen demand (COD) provides valuable insights into the biodegradability of organic compounds present in the solution over time (Rabab A. Hakami et al. 2024).

2. Experimental Framework

2.1. Reagents and Chemicals

Marbofloxacin ($C_{17}H_{19}FN_4O_4$, MW: 362 g/mol, purity: 99.7%) was obtained from Shanghai Industrial Company in China. Analytical-grade reagents were sourced from Shanghai Chemical Company, including hydrogen sulfate, potassium chloride, and ferrous sulfate heptahydrate ($FeSO_4 \cdot 7H_2O$, 99.8%). High-purity analytical standards A ($C_{13}H_8F_2N_2O_4$, MW: 294 g/mol), B ($C_{15}H_{15}O_4N_4F$, MW: 334 g/mol), and C ($C_{16}H_{17}O_4N_4F$, MW: 349 g/mol) were obtained from LGC Luckenwald in Germany. Fluka supplied additional reagents such as triethylamine, ammonium acetate, and sodium perchlorate, whereas acetonitrile (HPLC grade) and sodium sulfate were purchased from Sigma-Aldrich and Acros Organics. Titanium tetrachloride and sulfuric acid, required for preparing the titanium reagent for hydrogen peroxide quantification, had purities of 99.7% and 98.8%, respectively, and were procured from Acros. All aqueous solutions were prepared using ultrapure water from a Millipore MiliQ system at ambient temperature.

2.2. Electrochemical Setup

A Potentiostat/Galvanostat model PGZ 302 was employed to monitor and control the electrochemical reactions. The experiments were conducted in an open electrochemical cell with a capacity of 200 ml. The electrodes utilized included carbon felt (CF) (12 cm x 8 cm × 0.5 cm), carbon graphite, and a marbofloxacin solution at a concentration of 0.144 mM, all acquired from the French company Mersine. The anodic compartment was equipped with a platinum electrode spanning 5 cm^2, provided by PLATECXIS, France. The pH of the working solution was adjusted to 3.0 using a 0.10 mM H_2SO_4 solution. The investigation varied current densities, employing values of 50, 200, 300, and 400 mA to assess their effect on the degradation process.

2.3. Analytical Methodology

For the degradation experiments, marbofloxacin (hereinafter referred to as Marba) was solubilized in a 200 ml aqueous solution of 50 mM Na_2SO_4 to achieve a working concentration of 0.144 mM. It was supplemented with 0.2 mM Fe^{2+} as a catalyst. The reactions were carried out under ambient conditions. The temporal progression of Marba degradation and the accumulation of oxidation intermediates were monitored via High-Performance Liquid Chromatography (HPLC), utilizing a reversed-phase system from Merck Lachrom. Optimal detection was accomplished at a wavelength of 278 nm.

The chromatographic separation was conducted using an Agilent C18 thermal hypersil column (5 μm, 4.6 mm × 26 cm) interfaced with an "Empower 2" data logging software. The column was maintained at a temperature of 45°C throughout the analysis. The mobile phase comprised a mixture of methanol, KH_2PO_4, tetraethylammonium sulfate $[(CH_3(CH_2)_3)_4N]_2SO_4$, and H_2SO_4 in a volumetric ratio of 29:71 (v/v).

The Chemical Oxygen Demand (COD) reduction efficiency, a key indicator of mineralization, was quantified using dichromate-based COD measurement techniques. Samples for COD analysis were subjected to thermal digestion for two hours at 150°C in a COD VARIO photometer. The resultant COD values were then determined using spectrophotometry.

Ion chromatography (ICS-1000 from Dionex) was employed to identify inorganic ions generated during mineralization. An injection volume of 26 µL was used. The system was outfitted with an IonPac AG4A-CS (5 cm × 6 mm) column guard and an IonPac AS4A-CS (26 cm × 5 mm) analytical column to facilitate the identification of anions such as fluoride (F^-) and nitrate (NO_3^-). A mobile phase consisting of 1.7 mM sodium carbonate and 1.8 mM sodium bicarbonate was delivered at a 2.0 mL/min flow rate. For the cationic species, notably ammonium (NH_4^+), an IonPac CS12A (25 cm × 6 mm) cation-exchange column coupled with an IonPac CG12A (5 cm × 4 mm) guard column was utilized. The detection system, controlled by Chromeleon SE software, featured a DS6 detector with a heated cell set to 35°C, ensuring precise ion quantification.

3. Statistical Modeling Approaches for Electrochemical Degradation of Marbofloxacin

3.1. Modeling Strategies and Validation Criteria

Our research adopted a composite statistical modeling framework to delineate the electrochemical degradation kinetics of marbofloxacin. We developed five distinct statistical models, each tailored to elucidate the degradation kinetics' dependence on pivotal factors: temporal duration, applied current density, and cathode type (CT). These models were instrumental in decrypting the complex interactions and facilitating a nuanced understanding of the degradation process, essential for optimizing pharmaceutical water treatment methodologies.

The selected models span a gamut of observed degradation behaviors, capturing nonlinearities, interaction effects, and cathode-specific kinetic patterns. This comprehensive array of models was essential to decoding the degradation's mechanistic underpinnings and ascertaining the most efficacious operational parameters for degradation.

Our validation paradigm was anchored in rigorous statistical methods, including residual analysis for model fit assessment, tests for homogeneity of variance to ensure consistent variability across predicted values, and stringent checks for multicollinearity to preclude redundant predictors. The adoption of nonlinear regression techniques, the integration of polynomial terms, and the application of spline interpolations were pivotal in ensuring the fidelity of our models in representing the intricate, often curvilinear relationships inherent in electrochemical reactions.

The deployment of these statistical models paves the way for substantiating hypotheses in electrochemical degradation and bolsters the predictive acumen necessary for the proactive design of water treatment protocols.

3.2. Polynomial Modeling of Hydrogen Peroxide (H_2O_2) Production

The polynomial model is constructed by incorporating terms up to the third degree for both time (T) and electrical current (EC), along with an interaction term between these two variables. This choice is driven by the necessity to model the complex dynamics observed, including acceleration effects, deceleration, and interaction. The model equation is as follows:

$$H_2O_2 = \beta_0 + \beta_1 CE + \beta_2 CE^2 + \beta_3 CE^3 + \beta_4 T + \beta_5 T^2 + \beta_6 T^3 + \beta_7 (CE \times T) + \dot{n} \quad (4)$$

where:

- H_2O_2 denotes the concentration of hydrogen peroxide,
- EC represents the applied electrical current,
- T signifies time,
- β_0 to β_7 are the coefficients of the model to be estimated,
- ϵ is the error term, capturing the variability not explained by the model.

The quadratic (CE^2, T^2) and cubic (CE^3, T^3) terms facilitate modeling the nonlinearity of the relationship, while the interaction term ($CE \times T$) captures how the effect of time on H_2O_2 concentration varies with the level of EC.

3.3. Nonlinear Regression Model for Marbofloxacin Degradation Dynamics

To investigate the dynamics of marbofloxacin degradation in an aqueous solution, a nonlinear model was developed to assess the combined effect of *EC*, *CT*, and elapsed time (*t*) on the concentration of marbofloxacin (Mps). The degradation process was hypothesized to follow kinetics that could be influenced by the type of cathode used and the intensity of the applied *EC*. The model is formulated as follows:

$$\text{Marbo}(t) = (\alpha_{CG} + \gamma_1 \cdot CE) \cdot e^{(-\beta_{CG} \cdot t)} + (\alpha_{CF} + \gamma_2 \cdot CE) \cdot e^{(-\beta_{CF} \cdot t)} \quad (5)$$

Where α_{CG} and α_{CF} represent the initial marbofloxacin concentrations for the *CG* and CF cathode types, respectively, in the absence of *EC*. γ_{CG} and γ_{CF} represent the effect of the *EC* on the initial concentration for each *CT*, while β_{CG} and β_{CF} represent the degradation rates associated with each *CT*. This specification allows for estimating parameters that reflect variations in degradation kinetics, based on time and *EC* and *CT*. The parameter estimation was performed using nonlinear regression, allowing flexibility in modeling these complex relationships.

3.4. Generalized Linear Modeling (GLM) of Marbofloxacin Degradation Dynamics

We employed a Generalized Linear Model (GLM) utilizing a Gaussian family with an identity link function to investigate the impact of various operational parameters on the degradation of the pharmaceutical substance Marbofloxacin. This methodological choice allows for the direct modeling of Marbofloxacin concentration in relation to both continuous and categorical predictors, efficiently addressing the potential nonlinear relationships between these variables.

The model's construction was informed by preliminary data observations, indicating a nonlinear relationship between Marbofloxacin concentration and time, as well as the potential influence of catalyst concentration and the type of cathode used. To accurately capture the temporal complexity, cubic spline terms (T_spline1 and T_spline2) were incorporated, allowing the model to flexibly fit the observed phases of rapid decline followed by a plateau in Marbofloxacin concentration.

The variable Fe^{2+} catalyst_squared was introduced to examine the quadratic effect of catalyst concentration after noting that the relationship between Fe^{2+} catalyst and Marbofloxacin concentration did not follow a simple linear pattern. This transformation enabled precise modeling of the catalyzer's effect on Marbofloxacin concentration, accelerating at higher Fe^{2+} catalyst levels.

Lastly, the type of cathode (CT), represented as a categorical variable, was included to investigate its distinct effects on Marbofloxacin degradation.

The theoretical equation derived from our model is articulated as follows:

$$\hat{y} = \beta_0 + \beta_1 \times (Fe\ catalyst)^2 + \beta_2 \times T\_spline1 + \beta_3 \times T\_spline2 + \beta_4 \times CT_{CG} + \text{ñ} \quad (6)$$

where:

- ў represents the predicted concentration of Marbofloxacin,
- Fe^{2+} *catalyst squared* is the squared term of the catalyst concentration, included to account for the observed quadratic relationship between the catalyst concentration and Marbofloxacin degradation,
- *T_spline*1 and *T_spline*2 are spline terms derived from the time variable to model the nonlinear degradation pattern of Marbofloxacin over time, capturing both the rapid initial decrease and subsequent plateau phase,
- CT_{CG} is a dummy variable representing the effect of using the CG type cathode compared to the reference cathode type,
- β0, β1, β2, β3, and β4 are coefficients estimated by the model, quantifying the impact of each predictor on Marbofloxacin concentration,
- ϵ denotes the error term, capturing unexplained variation in Marbofloxacin concentration.

3.5. Robust Linear Regression Analysis for Marbofloxacin Mineralization Dynamics

This study aimed to model the mineralization of the pharmaceutical substance marbofloxacin, with mineralization serving as the dependent variable. Employing a robust linear regression model, we sought to quantify the degradation dynamics of marbofloxacin in an experimental setup.

The regression model was constructed using an ordinary least squares (OLS) approach, incorporating robust standard errors to enhance the model's resilience against the influence of outliers. This method improves the reliability of parameter estimates, especially in the presence of non-constant variance (heteroscedasticity) among residuals.

We specified the model to include a linear time variable ($T_{centered}$), a quadratic time variable $(T_{centered})^2$, and a categorical variable (CF_{dummy}) to differentiate between two cathode types used in the degradation process. Incorporating a linear and quadratic time term allows for modeling both the initial rate of degradation and its potential acceleration or deceleration over time. The CF_{dummy} variable captures the impact of CT on marbofloxacin mineralization, providing insight into the comparative efficiency of the cathodes.

The model also accounts for the EC as a control variable, acknowledging its critical role in the electrochemical process affecting marbofloxacin's degradation rate.

The final model was specified as follows to capture the relationship between the mineralization rate of Marbofloxacin and the experimental conditions:

$$COD(t) = \beta_0 + \beta_1 T_{centered} + \beta_2 T^2{}_{centered} + \beta_3 CE + \beta_4 CF_{dummy} + \text{ň} \quad (7)$$

Where Mps represents the mineralization of the pharmaceutical substance, $T_{centered}$ is the centered time variable, $T^2{}_{centered}$ is its squared term to capture potential nonlinearity, CE is the electric current, and CF_{dummy} is a dummy variable for the type of cathode used, with β_i representing the coefficients estimated by the robust regression model and ϵ the error term. We applied robust standard errors to account for heteroskedasticity and potential outliers. The model's adequacy was evaluated through a series of diagnostic tests, including but not limited to residual analysis, variance inflation factor (VIF) analysis for multicollinearity, and cross-validation where applicable.

3.6. Nonlinear Modeling of Instantaneous Current Efficiency (ICE) and Its Influences

A nonlinear statistical modeling approach was employed to elucidate the dynamic interplay between current intensity (CI), exposure time (Time), and the ICE while accounting for the influence of CT. Our model posits that ICE is not solely influenced linearly by CI and time, but also exhibits quadratic and exponential relationships.

The estimated model is articulated as follows:

$$ICE_i = \beta_0 + \beta_1 CI_i + \beta_2 CI_i^2 + \beta_3 e^{\beta_4 Time_i} + \beta_5 CT\_dummy1_i + \beta_6 (CI \times CT)_i + \beta_7 (Time \times CT)_i + \text{ň}_i \quad (8)$$

Where ICE_i denotes the ICE for observation i, CI_i represents the current intensity, $Time_i$ represents the exposure time, and CT_dummy1_i is an indicator variable reflecting the CT. The terms $(CI \times CT)_i$ and $(Time \times CT)_i$ are interaction terms between the CI and time variables with the CT. These terms introduce model flexibility to capture the potential modifying effects of the CT on the relationships between ICE, CI, and Time. $\beta_0, \beta_1, ..., \beta_7$ represent the estimated parameters, and ϵ_i is the error term for observation i. It is posited to follow a normal distribution with a mean of zero.

The nonlinear specification was predicated on electrochemical theory and preliminary exploratory data analysis, suggesting that the associations between ICE and its predictors did not adhere to a strictly linear form.

In this study, Stata version 16 was utilized for statistical modeling. Nonlinear models and complex relationships between variables were estimated using Stata's **nl** command, while polynomial models were fitted with the **regress** and **glm** commands. These functions enabled precise modeling of marbofloxacin degradation and ICE, considering a variety of operational parameters and electrochemical characteristics. All tests were two-tailed, and values of $p < 0.05$ were considered statistically significant.

4. Results and Discussion

4.1. Hydrogen Peroxide Production at Two Cathode Types

The study's primary objective was to examine the capability of carbon felt (CF) and carbon graphite (CG) cathodes to produce hydrogen peroxide (H_2O_2) during the electrochemical reduction of oxygen in a 50 mM Na_2SO_4 solution. The generation of H_2O_2 is significant, as outlined in Equation (9), due to its reaction with ferrous ions (Fe^{2+}) to produce hydroxyl radicals ($^{\bullet}OH$), which are essential in the Fenton process for degrading organic contaminants. Given the critical role of the cathode in H_2O_2 synthesis, highlighted by Equation (10), understanding its production across different cathode types is paramount.

The study's primary objective was to examine the capabilities of CF and CG cathodes in producing H_2O_2 during the electrochemical reduction of oxygen in a 50 mM Na_2SO_4 solution. The generation of H_2O_2 is significant, as outlined in Equation (9), due to its reaction with ferrous ions (Fe^{2+}) to produce hydroxyl radicals ($^{\bullet}OH$), which are essential in the Fenton process for degrading organic contaminants. Given the critical role of the cathode in H_2O_2 synthesis, highlighted by Equation (10), understanding its production across different cathode types is paramount (Brillas et al. 2009).

During the initial twenty minutes of electrolysis, there was a significant increase in H_2O_2 production, leading to a steady state as the formation rate (Equation (10)) matched the rate of H_2O_2 consumption and decomposition (Equations (11) and (12). At lower current densities of 50 mA and 100 mA, peak H_2O_2 levels were attained within 70 minutes, whereas at higher densities, a peak was reached within 40 minutes.

$$Fe^{2+} + H_2O_2 \rightarrow OH^- + Fe^{3+} + {}^{\bullet}OH \quad (9)$$

$$2H^+ + O_2 + 2e^- \rightarrow H_2O_2 \quad (10)$$

$$2H_2O_2 \rightarrow 2H_2O + O_2 \quad (11)$$

$$H_2O_2 \rightarrow HO_2 + H^+ + e^- \quad (12)$$

Figure 1 elucidates the comparative analysis of H_2O_2 generation over time for CF and CG cathodes under various current densities. The graph presents a comparative analysis of H_2O_2 generation over time for two different cathode materials, CF and CG, across various current densities. At lower current densities (50 and 100 mA), both cathodes demonstrate a steady increase in H_2O_2 concentration, indicative of efficient electrochemical reactions proceeding without reaching an apparent limiting threshold. This behavior suggests that the reaction sites are not saturated at these lower current densities, and competitive side reactions are minimized.

In contrast, a distinct pattern emerges at higher current densities (300 and 400 mA). After a swift initial rise, the concentration of H_2O_2 levels off or decreases, pointing to limiting mechanisms curtailing production. These may include the saturation of reactive sites, a slowdown in reaction kinetics, or losses due to secondary processes such as the catalytic decomposition of H_2O_2.

Comparing the high-current responses of CF and CG cathodes, the CF cathode displays a slightly more stable H_2O_2 concentration, potentially indicating higher resistance to limiting processes or better management of side reactions than the CG cathode. However, this advantage is modest, suggesting comparable performances of both cathode materials under the tested operational conditions (Qiango et al. 2002).

These findings underscore the importance of considering both CT and current density in designing H_2O_2 production systems to optimize efficiency and stability. The interpretation of these results should inform material selection for cathodes and the calibration of electrochemical parameters for industrial and environmental applications (Fig. 1).

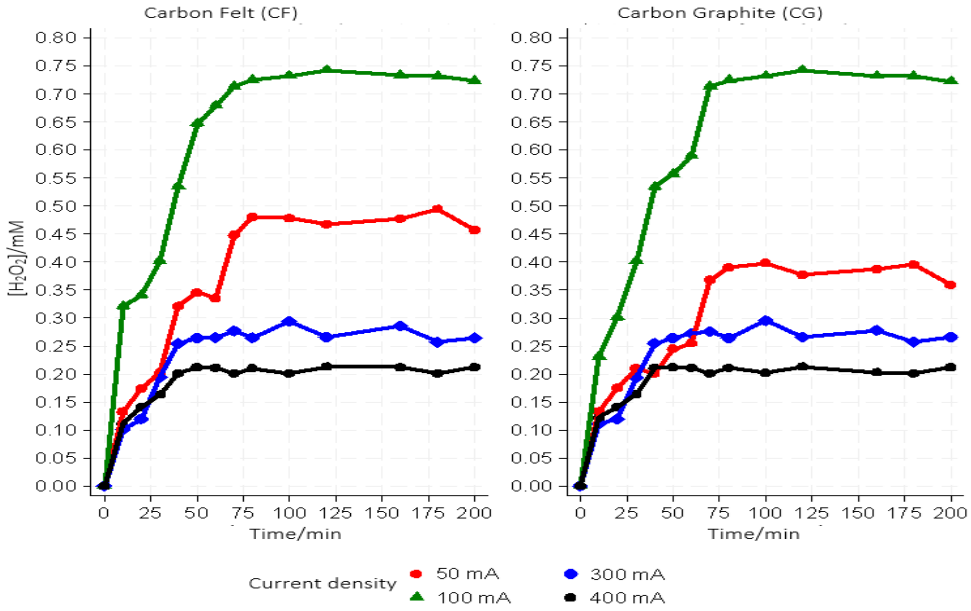

Fig. 1. Electrochemical Generation of H_2O_2: Comparative Dynamics Across Carbon Felt and Graphite Carbon Cathodes at Varied Current Intensities

This investigation's polynomial model reflects the nonlinear relationships between time, EC, and H_2O_2 concentration. The data revealed an initial rise in H_2O_2 levels, subsequently plateauing. This stabilization level appeared dependent on the EC applied, with a more pronounced plateau observed at lower currents. Given these nuances, a standard linear model was deemed insufficient, leading to adopting a polynomial model capable of integrating both linear and nonlinear effects and variable interactions. This polynomial model has highlighted the nonlinear effects of EC. By incorporating linear, quadratic, and cubic terms for CE, it showcases a complex relationship that underscores the nonlinear impact of EC on H_2O_2 concentration.

The nuanced modeling reveals an initial concentration increase that approaches a saturation point as EC levels rise. Specifically, the linear EC term (β_1 = 0.0138922, $p < 0.0001$) indicates a positive relationship with H_2O_2 concentration, while the quadratic (β_2 = -0.0000668, $p < 0.0001$) and cubic ($\beta_3 = 8.87e^{-08}$, $p < 0.0001$) terms elucidate the deceleration and subsequent complexity of this relationship at higher EC values. Similarly, the coefficients associated with time articulate an increase in H_2O_2 concentration, eventually trending toward stabilization. The progression from a linear increase (β_4 = 0.0103325, $p < 0.0001$), through a decelerating phase (β_5 = -0.00007, $p < 0.0001$), to a resurgence in growth at extreme time values ($\beta_6 = 1.66e^{-07}$, $p < 0.0001$), highlights both the critical role of time and its intricate contribution to the observed dynamics. Furthermore, the interaction term between EC and T further underscores the need to consider the combined effects of EC and time. The negative interaction ($\beta_7 = -5.08e^{-06}$, $p < 0.0001$) indicates that the joint increase of EC and T moderates H_2O_2 concentration growth, suggesting that the synergy of these variables influences H_2O_2 concentration differently compared to their isolated effects (Table 1, Eq. 13).

$$H_2O_2 = -0.5808354 + 0.0138922 \cdot CE - 0.0000668 \cdot CE^2 + 8.87 \cdot 10^{-8} \cdot CE^3 + 0.0103325 \cdot T - 0.00007 \cdot T^2 + 1.66 \cdot 10^{-7} \cdot T^3 - 5.08 \cdot 10^{-6} \cdot CE \cdot T \quad (13)$$

Table 1. Polynomial Model Results for H_2O_2 Concentration (Model 1)

Variable	B	Std. err.	t Stat.	p-value	95%CI
EC	0.0138922	0.0007673	18.11	<0.0001	[0.0123707, 0.0154137]
$(EC)^2$	-0.0000668	$3.68e^{-06}$	-18.13	<0.0001	[-0.0000741, -0.0000595]
$(EC)^3$	$8.87e^{-08}$	5.12e-09	17.33	<0.0001	[$7.86e^{-08}$, $9.89e^{-08}$]
Time	0.0103325	0.0007602	13.59	<0.0001	[0.008825, 0.01184]
$(Time)^2$	-0.00007	$9.51e^{-06}$	-7.36	<0.0001	[-0.0000889, -0.0000512]
$(Time)^3$	$1.66e^{-07}$	$3.24e^{-08}$	5.13	<0.0001	[$1.02e^{-07}$, $2.31e^{-07}$]
EC x Time	$-5.08e^{-06}$	$6.30e^{-07}$	-8.07	<0.0001	[$-6.33e^{-06}$, $-3.83e^{-06}$]
Intercept	-0.5808354	0.0421223	-13.79	<0.0001	[-0.6643655, -0.4973053]
Model Fit: R-squared = 92.33%, Adjusted R-squared = 91.82%					

4.2. Impact of Applied Current, Catalyst Fe^{2+} Amount, and Type of Cathode on Marba's Degradation Rate

Using the electro-Fenton method, the oxidative breakdown of Marba was carried out in an electrolytic cell with a 200 ml capacitance at various current densities of 50-400 mA by examining the samples taken at regular intervals using HPLC.

Since CF and CG are the two types of carbon cathodes, Fig. 2 shows how the current affects the oxidative movement of the Marba pollutant. Due to the increased generation of hydroxyl ions and the subsequent electrochemical reactions that produce peroxide (as shown in Equation 2), as well as the faster synthesis of $^{\bullet}OH$/M on the anode's surface (as shown in Equation 6), the rate of Marba's breakdown increases with the current. The significance of Fig. 2 in understanding the breakdown of Marba becomes evident. According to these findings, the breakdown process follows first-order pseudo-kinetics. Furthermore, Fig. 3 shows that the two investigated cathodes have optimal current densities of 300 mA for the breakdown of Marba. As previously indicated, higher concentrations of H_2O_2 were achieved at current densities of 200 mA and 50 mA. These conclusions are supported by Equation 9. Equation 10 describes how a minimum amount of peroxide in the solution hinders electrochemical reactions and the breakdown process. Equation 14 illustrates how anodic oxidation produces $^{\bullet}OH$, thereby facilitating the oxidation of Marba.

$$H_2O + Pt \rightarrow e^- + Pt(^{\bullet}OH) + H^+ \quad (14)$$

The graph presents the degradation profile of marbofloxacin over time under different current intensities, categorized by the type of cathode used: CF and graphite carbon (CG). The degradation curves indicate a swift reduction in marbofloxacin concentration across all current settings, with the steepest decline occurring within the initial period.

For the CF cathode, the marbofloxacin concentration decreases rapidly and then levels off, with the lowest current (50 mA) showing a marginally more gradual descent compared to higher currents. This suggests that while the CF cathode is effective at initiating marbofloxacin degradation, the degradation rate does not substantially increase with higher current intensities beyond a certain threshold.

In contrast, the CG cathode shows a notably different pattern of degradation. Although all currents achieve a significant reduction, the concentrations at 50 mA and 200 mA display a less steep decline compared to 300 mA and 400 mA. This suggests a complex relationship exists between the applied current and the degradation efficiency of the graphite material.

The uniformity of the degradation paths after the initial drop hints at a possible rate-limiting step that is not solely dictated by CI but could also be influenced by the characteristics of the cathode material itself. Notably, when considering both cathode types at 400 mA, the curves tend to flatten earlier than lower currents, indicating a rapid approach to a degradation limit or equilibrium state.

This graphical representation underscores the necessity of optimizing operational parameters, such as the selection of cathode material and the adjustment of CI, to enhance the electrochemical degradation process for contaminants like marbofloxacin in aqueous solutions. The data suggests that while both CF and CG cathodes are effective, their performance can be fine-tuned with precise current adjustments to achieve optimal degradation rates (Fig. 2).

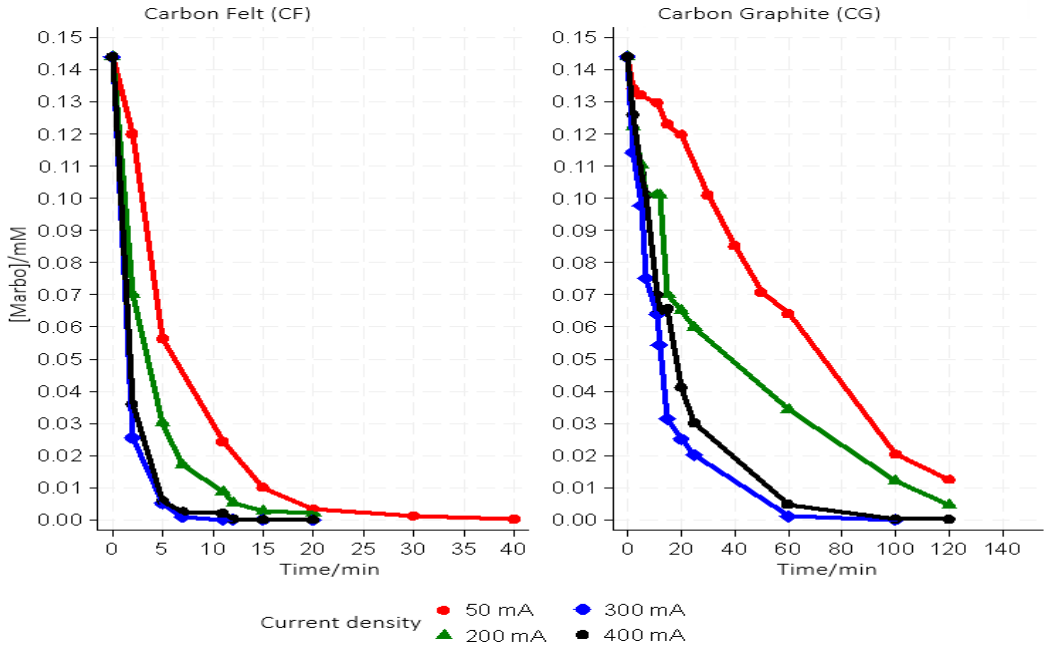

Fig. 2. Marbofloxacin Degradation Efficiency: Comparative Analysis between Carbon Felt and Graphite Cathodes under Variable Currents

The ln(C0/Ct) versus time graphs for CF and CG cathodes show distinct degradation behaviors under different current densities. Specifically, the CF cathode shows a significant and abrupt ln(C0/Ct) increase, particularly at 300 and 400 mA current densities. This observation suggests a rapid progression of the reaction, resulting in a substantial decrease in the concentration of the reactant within a short period.

Conversely, the CG cathode shows a more gradual increase in ln(C0/Ct) across equivalent current ranges, indicating a slower degradation than the CF cathode. It is worth noting that at a current of 50 mA, the CG curve shows the least steep slope, indicating a gradual decrease in substance concentration. This difference between the CF and CG profiles suggests inherent variations in the properties of the cathodes or the reaction mechanisms they facilitate.

These kinetic insights yield a valuable understanding of the influence of electrochemical conditions on substance stability. The analysis underscores the effectiveness of electrochemical methods for chemical degradation and highlights the significance of selecting an appropriate cathode and current density to tailor the degradation rate and process efficiency.

A detailed interpretation of these findings is crucial for optimizing operational parameters in practical applications such as wastewater treatment and pharmaceutical contaminant decontamination, where controlled degradation of pollutants is of utmost importance (Fig. 3).

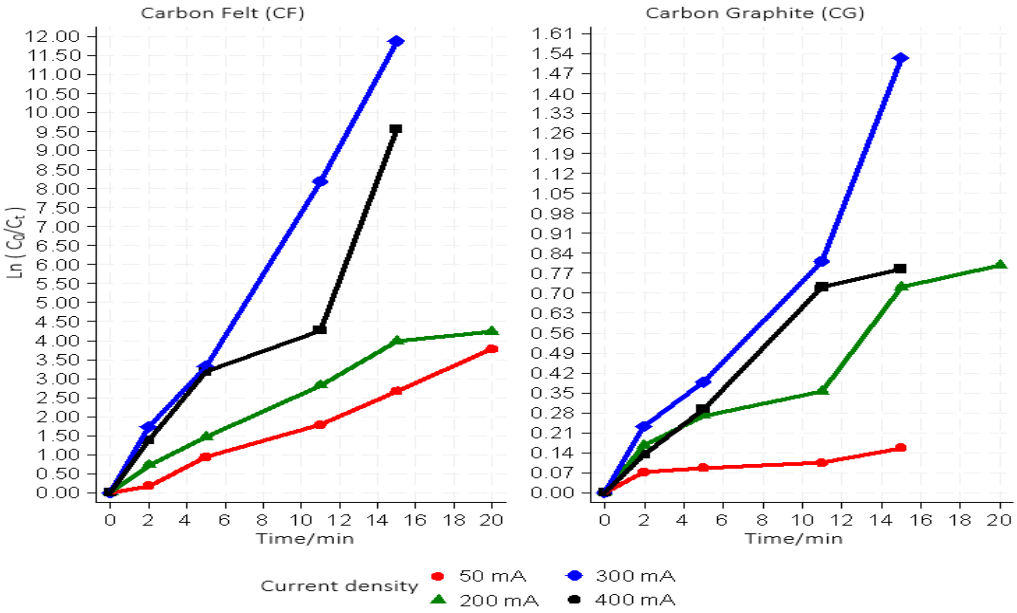

Fig. 3. Comparative Analysis of Marbofloxacin Degradation Kinetics under Varied Current Densities: Influence of CF and CG Cathodes. Employing Conditions: Fe^{2+} Catalyst Concentration at 0.1 mM, Initial [Marbo] at 0.144 mM, [Na_2SO_4] at 50 mM, Volume of 200 mL, at pH 3, and Ambient Temperature

However, elevating the current density above 300 mA causes Marba's degradation kinetics to slow down and has no discernible impact on the pollutant's oxidation process. Equations (10 and 15) illustrate how parasitic processes during electrochemical oxidation enhance waste, which might be one reason for this behavior. Equation (5) illustrates how Pt (•OH) and Equation (16) fight with the anode's ability to produce O_2 (Yahyaet al. 2023).

$$H_2O_2 + 2H^+ + 2e^- \rightarrow 2H_2O \quad (15)$$

$$2^{\bullet}OH \rightarrow H_2O_2 \quad (16)$$

The rate constants for the breakdown of Marba were calculated using $\ln(C_0/C_t)$ by assessing the cathodes under investigation's efficiency, as shown in Fig. 3. First-order pseudo-kinetics was the underlying assumption used in the computations. Notably, a methodical approach was taken to find the optimal current density, which produces the largest rate constant. The data clearly show that there is an increase in the rate constant with increasing current on the cathode material until the applied current reaches its ideal value, as shown in Fig. 2. Based on the previously described findings, it is evident that the cathode of CF, as opposed to CG, has larger rate constants than carbon graphite, making it more effective for the oxidative breakdown of the organic pollutant Marba.

To explore the dynamics of marbofloxacin degradation, a nonlinear model was constructed to examine the combined effect of EC, CT, and elapsed time (t) on the concentration of marbofloxacin (Mps). It was assumed that the degradation followed kinetics that could be modified by the type of cathode used and the intensity of the applied EC. The nonlinear model analysis of marbofloxacin degradation revealed that the estimated initial concentration of marbofloxacin for the CG-type cathode indicates a significant amount present before the start of electrochemical degradation ($\beta_1 = 0.167006$, $p < 0.001$). Interestingly, for this CG cathode, the EC was found to have a negative effect on the initial concentration ($\beta_2 = -0.0001715$, $p < 0.001$), implying that higher currents lead to a reduced initial marbofloxacin concentration, which suggests an increase in the degradation rate. This is further corroborated by the substantial decay rate of marbofloxacin with the CG cathode ($\beta_3 = 0.271033$, $p < 0.001$), highlighting the rapid kinetics of its degradation. On the other hand, the initial concentration of marbofloxacin associated with the CF-type cathode was also significantly impacted ($\beta_4 = 0.1709255$, $p < 0.001$), indicating the cathode type's distinct influence on the degradation process. Although the effect of EC on the initial concentration with the CF cathode showed a trend towards significance ($\beta_5 = -0.0001252$, $p = 0.062$), it indicated a possible but less pronounced relationship compared to the CG cathode. Moreover, the decay rate for the CF cathode suggests a varied degradation rate ($\beta_6 = 0.3597625$, $p < 0.001$), hinting that the cathode's nature markedly influences marbofloxacin's degradation dynamics (Table 2, Eq. 17).

$$Marbo(t) = (0.167006 + (-0.0001715 \times CE)) \times e^{(-0.271033 \times t)} + (0.1709255 + (-0.0001252 \times CE)) \times e^{(-0.3597625 \times t)} \quad (17)$$

Table 2. Estimated Parameters of the Marbofloxacin Degradation Model (Model 2)

Variable	B	Std. err.	t Stat.	p-value	95%CI
Initial Concentration CG (α_1)	0.16700	0.0106307	15.71	<0.001	[0.14582, 0.18819]
Electric Current Effect CG (γ_1)	-0.00017	0.0000342	-5.02	<0.001	[-0.00023, 0.00010]
Decay Rate CG (β_1)	0.027103	0.0033209	8.16	<0.001	[0.20484, 0.3372]
Initial Concentration CF (α_2)	0.17093	0.018426	9.28	<0.001	[0.13420, 0.20764]
Electric Current Effect CF (γ_2)	-0.00013	0.0000661	-1.89	0.062	[-0.0003, 6.50e-06]
Decay Rate CF (β_2)	0.359762	0.0538019	6.69	<0.001	[0.25253, 0.46698]
Model fit: R-squared = 94.18%, Adjusted R-squared = 93.71%					

Moreover, the effect of the Fe^{2+} catalyst concentration (mM) on Marba's oxidative breakdown was examined. The effects of using various catalyst concentrations (0.05, 0.1, and 0.2 mM) for the CF and CG cathodes with an applied current of 300 mA are shown in Figs. 4 and 5. It was found that the rate at which the organic pollutant underwent oxidative breakdown increased in tandem with the concentration of the catalyst. More specifically, the rate of oxidative degradation increased from 0.05 to 0.1 mM.

The graph presents the degradation rate of marbofloxacin over time for two cathode types, CF and CG, with three different concentrations of iron-based (Fe^{2+}) catalysts.

Across both cathode types, a marked initial decrease in marbofloxacin concentration indicates a strong initial catalytic activity. This activity appears to be more pronounced with higher concentrations of the Fe^{2+} catalyst, as evidenced by the steeper descent of the curves for 0.1 mM and 0.2 mM compared to 0.05 mM.

The curve for the CF cathode demonstrates that the highest Fe^{2+} catalyst concentration (0.2 mM) leads to the fastest degradation of marbofloxacin, with the curve plummeting rapidly before stabilizing. This may suggest that a catalytic saturation is reached or that the system is approaching a dynamic equilibrium where the degradation rate encounters limits.

For the CF or CG cathode, while the degradation pattern is similar, the curve for 0.2 mM seems to show a slightly longer active degradation period before reaching a plateau. This might be due to a different interaction between the marbofloxacin and the CG cathode surface or a different reactivity dynamic with the Fe^{2+} catalyst.

In both scenarios, it is evident that the Fe^{2+} catalyst concentration plays a pivotal role in the reaction kinetics of degradation. The findings underscore the significance of selecting an optimal catalyst concentration for effective degradation, with considerations needed for the specific properties of the cathode used within the electrochemical system (Fig. 4).

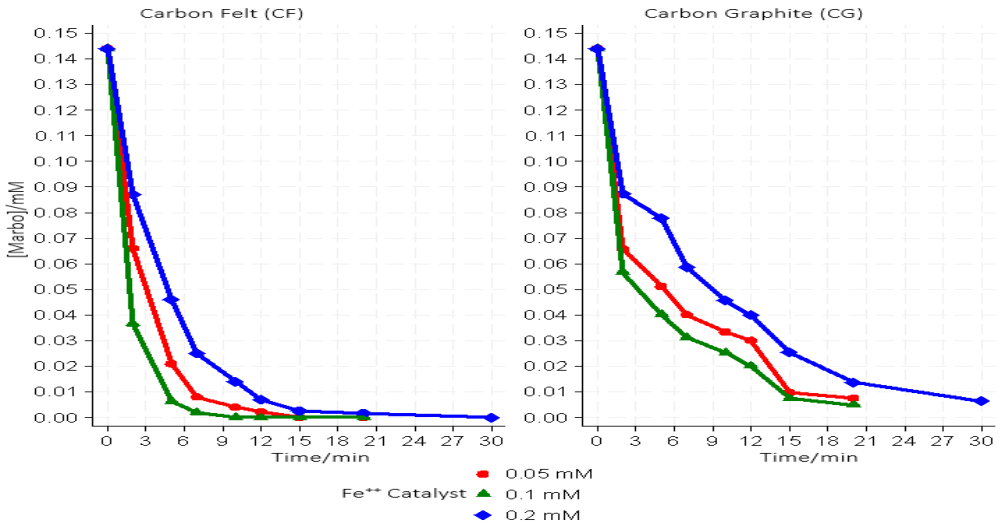

Fig. 4. Impact of Fe^{2+} Catalyst Concentration on the Degradation Rates of Marbofloxacin Using Carbon Felt and Graphite Cathodes Under Specific Conditions. Parameters: Applied Current of 300 mA, Initial Marbofloxacin Concentration of 0.144 mM, [Na_2SO_4] of 50 mM, Reaction Volume of 200 mL, at a pH of 3, and Ambient Temperature

The kinetic investigations depicted in the ln(C0/Ct) vs. time graphs articulate the nuanced impact of Fe^{2+} catalyst concentrations on marbofloxacin degradation across CF and CG cathodes. Notably, the catalyst's concentration demonstrates a nonlinear correlation with degradation efficacy. Sub-optimal concentrations of

0.1 mM and especially 0.05 mM Fe display unexpectedly superior kinetic enhancement, as evidenced by the pronounced steepness in ln(C0/Ct) values, particularly with the CF cathode. This suggests an optimal catalytic interplay at these lower concentrations, which may be attributed to improved electrochemical interactions and active site accessibility. The CG cathode follows this trend, albeit with a less aggressive profile, indicating a dependency of the degradation kinetics on the nature of the cathode material in addition to the catalyst concentration. These observations underscore the importance of fine-tuning Fe^{2+} catalyst concentrations to optimize degradation rates for targeted electrochemical applications, providing valuable insights for developing cost-effective and environmentally sustainable water treatment processes (Fig. 4).

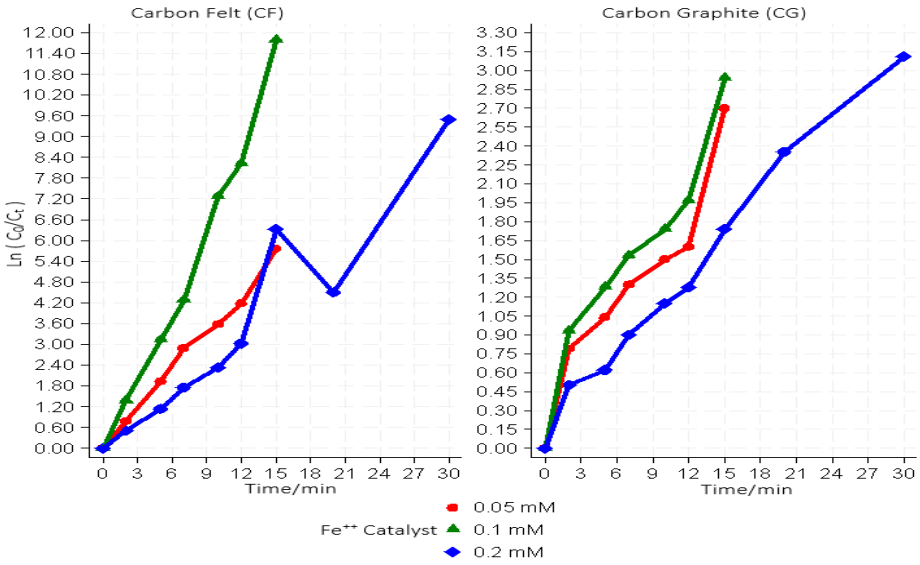

Fig. 5. Influence of Fe^{2+} Catalyst Concentration on Marbofloxacin Degradation Kinetics under Varied Currents with CF and CG Cathodes. Conditions: Applied Current of 400 mA, Initial Marbofloxacin Concentration of 0.144 mM, Sodium Sulfate [Na_2SO_4] at 50 mM, Volume of 200 mL, at pH 3, and Ambient Temperature

Furthermore, our Generalized Linear Model (GLM) analysis highlighted the key factors influencing Marbofloxacin degradation. The results from the cubic spline terms for time (**T_spline1** and **T_spline2**) confirmed a pronounced nonlinear relationship between time and Marbofloxacin concentration, with p-values below 0.001 for both terms.

Specifically, the **T_spline1** term showed a substantial negative effect on Marbofloxacin (β_1 = -0.0121, $p < 0.001$), while **T_spline2** exhibited a positive effect (β_2 = 0.0086, $p < 0.001$), indicating complex dynamics in the time-concentration relationship. Furthermore, the **CG** cathode type was significantly associated with an increase in Marbofloxacin concentration compared to the reference category (β_3 = 0.0180, p = 0.001), highlighting the impact of the cathode material on the degradation process.

The quadratic term for catalyst concentration (**Fe^{2+} catalyst_squared**) was also significant (p = 0.036), with a coefficient of 0.3575. This suggests that the effect of catalyst concentration on Marbofloxacin concentration increases at an accelerated rate as the catalyst concentration rises. This finding reinforces the notion that catalytic conditions are crucial for the effective treatment of pharmaceutical contaminants (Table 3, Eq. 18).

$$\hat{y} = 0.0993 + 0.3575 \times (Fe\ catalyst)^2 - 0.0121 \times T\_spline1 + 0.0086 \times T\_spline2 + 0.0180 \times CT_{CG} \quad (18)$$

Table 3. GLM Results for Marbofloxacin Degradation Factors

Marbofloxacin	β	Std. err.	t Stat.	p-value	95%CI
$(Fe\ catalyst)^2$	.3574988	.1705109	2.10	0.036	[0.0233, 0.6917]
T_spline1	-.0120845	.0010108	-11.96	<0.001	[-0.0141, -0.0101]
T_spline2	.008584	.0010766	7.97	<0.001	[0.0065, 0.0107]
CT_{CG}	.0179647	.0054883	3.27	<0.001	[0.0072, 0.0287]
Intercept	.0993318	.0073074	13.59	<0.001	[0.0850, 0.1137]
Model fit: log likelihood = 128.80; AIC = -4.952, BIC = -176.024					

4.3. The Applying Current's Effect and Type of Cathode on the Mineralization of Marbofloxacin

We carried out a mineralization experiment to evaluate the effectiveness of the electrical Fenton process for the organic contaminant Marba. The experiment involved currents ranging from 50 to 400 mA, using the same parameters as the oxidative degradation processes. We added Na_2SO_4 at a concentration of 50 mM, with the catalyst concentration fixed at 0.1 mM. The results of the COD removal process for the two cathodes in question are shown in Fig. 6. It is clear that the effectiveness of COD removal is comparable to the results of the oxidative decomposition trials. The use of the CF cathode with a current density of 300 mA yielded the highest mineralization efficiency (COD elimination) of 90% after six hours.

The graph depicts the reduction in Chemical Oxygen Demand (COD) over time during the electrochemical mineralization of marbofloxacin, analyzed for both CF and CG cathodes at varying current densities.

A clear trend emerges across both cathode types: the COD decreases significantly over time, suggesting the progressive mineralization of marbofloxacin. At all current densities, the reduction is rapid initially, followed by a more gradual decrease. This initial rapid decline indicates the swift onset of the electrochemical reaction leading to the breakdown of organic compounds.

For CF cathodes, the curves suggest that higher currents initially accelerate the mineralization process, as seen by the steeper slopes at 300 mA and 400 mA compared to 50 mA and 100 mA. This indicates that increasing the current density can enhance the mineralization rate, at least in the early stages.

Conversely, the highest current density of 400 mA for CG cathodes does not result in the steepest initial decrease. This observation may point to different electrochemical dynamics compared to the CF cathode. Instead, the 300 mA current density exhibits a more pronounced initial decline. This finding potentially indicates an optimal current density range for the CG cathode, maximizing marbofloxacin mineralization efficiency.

The gradual convergence of the curves at later times suggests that the difference in mineralization rates diminishes as the reaction proceeds. This convergence could be attributed to several factors, including the depletion of readily degradable marbofloxacin, the accumulation of intermediates, or reaching the limits of the electrochemical system's capacity.

This data underscores the importance of optimizing current density and cathode material selection to enhance the electrochemical treatment process for pharmaceutical contaminants. The variation in COD reduction patterns between CF and CG cathodes also highlights the potential for material-specific characteristics to influence the mineralization kinetics and overall efficiency.

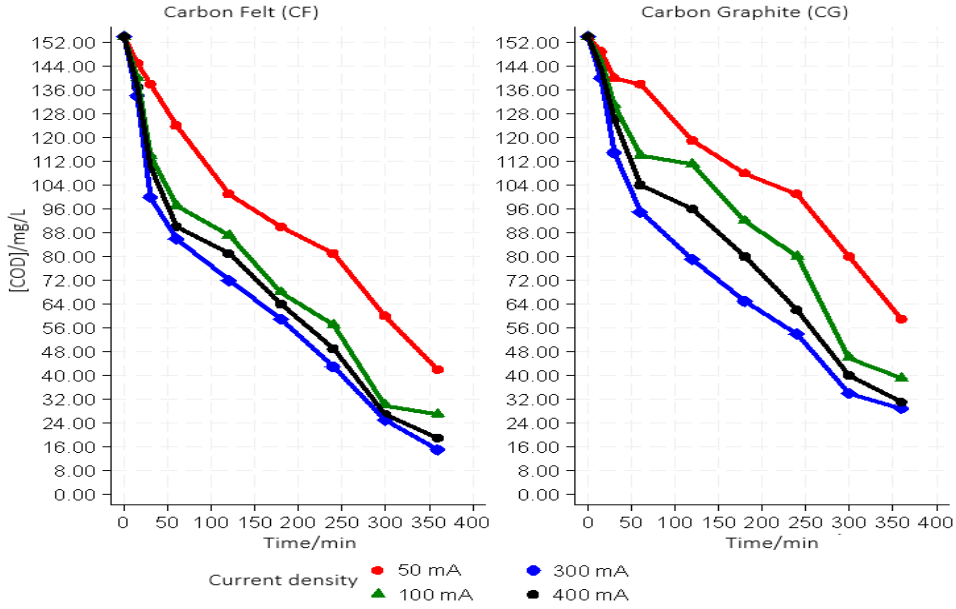

Fig. 6. Trends in COD Reduction for Marbofloxacin Mineralization Using CF and CG Cathodes. Experimental Parameters: [Marbo] at 0.144 mM, Fe^{2+} Concentration of 0.1 mM, [Na_2SO_4] at 50 mM, Volume of 200 mL, pH 3, and Ambient Temperature

After six hours, however, the CG cathode demonstrated 81% effectiveness in COD (mineralization) removal. At a current of 400 mA, the COD removal efficiency for the mineralization of the Marba solution was nearly identical to the value found at a current of 300 mA. Nonetheless, it is important to note that applying currents higher than 300 mA did not improve mineralization efficiency (Fig. 6).

Robust modeling of marbofloxacin mineralization reveals a significant and decreasing effect of time on COD reduction, averaging a decrease of 0.335 mg/L for each time unit (β_1 = -0.3352783, $p < 0.001$). The decline, however, is not uniformly linear, as the positive quadratic term suggests variability in the rate of COD degradation over time (β_2 = 0.0004617, $p < 0.001$). Concurrently, electric CI significantly influences mineralization, with each unit increase in current leading to a notable decrease in COD levels (β_3 = -0.0617981, $p < 0.001$), highlighting the critical role of electrochemical treatment in the mineralization process. Furthermore, the cathode type also dictates the pace of mineralization, with the CF type resulting in a more substantial COD reduction (β_4 = -12.0556, $p < 0.001$) compared to the CG type. The predictive strength of the model is underscored by an impressive R-squared value of 0.9260, confirming that it captures the majority of the variability in marbofloxacin mineralization. The model's overall validity is further corroborated by an F-statistic of 410.50 ($p < 0.001$), which demonstrates a strong correlation between the predictors and the observed response, thus highlighting the model's reliability in characterizing the underlying mechanisms of marbofloxacin degradation (Table 4, Eq. 19).

$$COD(t) = 104.92 - 0.34 \times T_{centered} + 0.00046 \times T^2_{centered} + 0.62 \times CE + 0.0056 \times CF_{dummy} \quad (19)$$

Table 4. Robust Linear Regression Results for Marbofloxacin Mineralization (MM)

Robust					
MM	B	Std. err.	t Stat.	p-value	95%CI
$T_{centered}$	-.3352783	.0134083	-25.01	p<0.001	[-0.362, -0.309]
$(T_{centered})^2$	.0004617	.000106	4.36	p<0.001	[0.000250, 0.000673]
EC	-.0617981	.0094913	-6.51	p<0.001	[-0.081, -0.043]
CF_{dummy}	-12.05556	2.803175	-4.30	p<0.001	[-17.651, -6.460]
Intercept	104.9198	3.909718	26.84	p<0.001	[97.116, 112.724]
Model fit: R-squared = 92.60%; (F-statistic = 410.50, $p < 0.001$); RMSE = 12.18					

One essential metric in the electrochemical process is the ICE.

This metric was computed for each cathode using the following Equation (20) to compare the current efficiency of the two cathode types under investigation:

$$ICE = \frac{(CODo - CODt) \times FV}{8It} \quad (20)$$

The constant of Faraday (96.487 C/mol) is represented by (F), COD0 represents the initial value of COD, the final value of COD is represented by CODt, the length of treatment is represented by (t), the volume of solution is represented by (V), and the current applied is represented by (I) in ampere.

Results derived from the mineralization data values displayed in Fig. 7 are derived from Fig. 6. The graph illustrates the ICE in the electrochemical treatment process of marbofloxacin with CF and CG cathodes over time, under various current densities.

ICE, a measure of the effectiveness with which EC is utilized to degrade contaminants, is depicted for both cathode types. It is apparent that ICE peaks early in the treatment process for both CF and CG cathodes, reflecting the highest efficiency near the start of the electrochemical reaction.

The highest ICE is observed at 50 mA for the CF cathode, suggesting optimal current utilization at this density. However, as the current density increases, ICE decreases, indicating a less efficient use of current for marbofloxacin degradation at higher current levels.

In contrast, ICE peaks at a higher current density of 100 mA for the CG cathode, hinting at a different electrochemical behavior than the CF cathode. The ICE at 300 mA and 400 mA for CG displays less variation, maintaining a more consistent current efficiency level throughout the process.

Both cathodes show a general trend of declining ICE over time, suggesting either a decreasing rate of marbofloxacin degradation as the concentration of the contaminant reduces or, perhaps, a shift in the electrochemical mechanisms active during different stages of the process.

The observed patterns highlight the intricate relationship between cathode material, current density, and treatment efficiency. They emphasize the need to calibrate these parameters to optimize the electrochemical degradation process, taking into account the specific characteristics of the cathodes and the dynamics of the EC applied (Fig. 5).

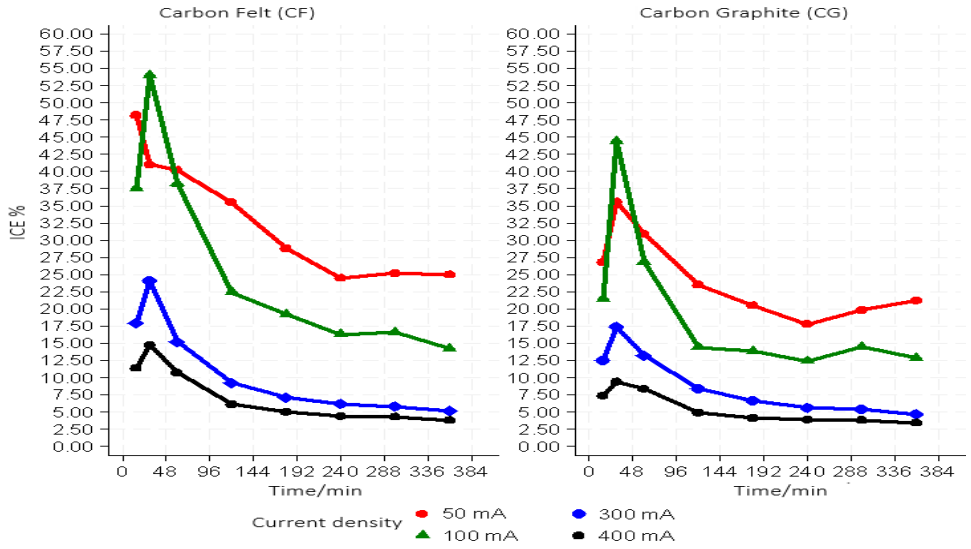

Fig. 7. ICE Profiles for Marbofloxacin Degradation: A Comparative Analysis Using Carbon Felt and Graphite Cathodes. Parameters: [Marbo] at 0.144 mM, Fe^{2+} Concentration of 0.1 mM, [Na_2SO_4] at 50 mM, Volume of 200 mL, at pH 3, and Ambient Temperature

After six hours, however, the CG cathode demonstrated 81% effectiveness in COD (mineralization) removal. At a current of 400 mA, the COD removal efficiency for the mineralization of the Marba solution was nearly identical to the value found at a current of 300 mA. Nonetheless, it is important to note that applying currents higher than 300 mA did not improve mineralization efficiency (Fig. 6).

Robust modeling of marbofloxacin mineralization reveals a significant and decreasing effect of time on COD reduction, averaging a decrease of 0.335 mg/L for each time unit (β_1 = -0.3352783, $p < 0.001$). The decline, however, is not uniformly linear, as the positive quadratic term suggests variability in the rate of COD degradation over time (β_2 = 0.0004617, $p < 0.001$). Concurrently, electric CI significantly influences mineralization, with each unit increase in current leading to a notable decrease in COD levels (β_3 = -0.0617981, $p < 0.001$), highlighting the critical role of electrochemical treatment in the mineralization process. Furthermore, the cathode type also dictates the pace of mineralization, with the CF type resulting in a more substantial COD reduction (β_4 = -12.0556, $p < 0.001$) compared to the CG type. An impressive R underscores the predictive strength of the model.

The nonlinear analysis of factors influencing the ICE reveals a series of complex interactions that are significantly modulated by CI and time while also being influenced by the type of cathode used. This analysis unveils a complex dynamic where CI is inversely correlated with the ICE (β_1 = -1.048, $p < 0.001$), indicating a decrease in efficiency as the current increases. However, this relationship is nuanced by the emergence of a slightly positive curvature as the current increases, as suggested by the positive quadratic term (β_2 = 0.0001158, $p = 0.046$). Time impacts efficiency exponentially, revealing an initial increase in efficiency, which tends to decrease as time progresses (β_3 = 16.11109).

By integrating the type of cathode into our model, we find that the CF-type cathode alters the effect of CI on efficiency, which is manifested by a significant interaction (β_4 = -0.212683, $p = 0.014$). Similarly, the interaction of time with the CF-type cathode reveals a distinct influence on efficiency (β_5 = -0.204935, $p = 0.043$), unlike the GC-type cathode, which serves as a reference. These interactions highlight the crucial role of the CT in evaluating and optimizing electrolytic efficiency.

In addition, the model shows remarkable robustness, as highlighted by an R-squared of 86.84%, indicating a substantial explanation of the variance in the instantaneous efficiency of electrolysis (IE) by the model variables. The adjusted R-squared, settling at 85.20%, confirms the relevance of the chosen predictors, even after adjusting for the number of variables included, affirming the statistical solidity of our model (Table 5, Eq. 21).

$$ICE = 23.82738 - 1.048129 \times CI + 0.0001158 \times CI^2 + 16.11109 \times e^{-0.0696978 \times Time} - 0.212683 \times CI \times CF - 0.204935 \times Time \times CF \quad (21)$$

Table 5. Nonlinear Regression Results for ICE

Variable	Coefficient	Std. Error	t-Statistic	p-value	95% CI
Intercept	23.82738	3.019009	7.89	<0.001	[17.77958, 29.87518]
CI	-1.048129	0.025869	-4.05	<0.001	[-1.15663, -0.9396233]
$(CI)^2$	0.0001158	0.0000567	2.04	0.046	[2.19e-06, 0.0002294]
Exp (Time)	16.11109	2.656464	6.06	<0.001	[10.78955, 21.43262]
CI x CF CT	-0.212683	0.083825	-2.54	0.014	[-0.38080, -0.0445595]
Time x CF CT	-0.204935	0.099065	-2.07	0.043	[-0.39908, -0.0107863]
Model Fit: R-squared = 86.84%, Adjusted R-squared = 85.20%, Root MSE = 4.797904					

All cathodes show very high initial ICE% values at low currents that diminish with increasing current and time. A slower rate of COD removal results from a reduction in the reaction rate with $^{\bullet}OH$ as the electrolysis process goes on and the amount of organic matter in the solution drops. It is evident from Fig. 7 that the CF cathode outperforms the CG cathode in terms of COD (mineralization) removal from the Marbo solution. In contrast to the CG cathode, the proportion of ICE declines with time but stays greater (Beqqal et al. 2017).

However, side reactions such as the evolution of hydrogen at the cathode and oxygen at the anode can also result in the loss of electrical energy, which might account for the low ICE% values for high currents Eqs. (22) and (23). This is in addition to H_2O_2 breakdown on electrodes (Brillas et al. 2009, Qiango et al. 2002).

$$H_2O + M^+ \rightarrow M(^{\bullet}OH) + H^+ + e^- \quad (22)$$

$$2\,M(^{\bullet}OH) \rightarrow 2\,M + O_2 + 2H^+ + 2\,e^- \quad (23)$$

The samples subjected to HPLC analysis during the initial (11) minutes of electrolysis demonstrated the progressive elimination of Marba and the emergence of many intermediates (Fig. 9). The chromatograms obtained from HPLC (Fig. 9) demonstrate how the concentration of these intermediates initially increases to a maximum and then progressively decreases until they are no longer detectable. HPLC identified intermediates A, B, and C by comparing their retention durations to standards and using UV spectra Fig. 8. When intermediates (polyhydroxylated or quinoid forms) reach higher oxidation states, they become unstable and undergo oxidative ring-opening reactions, resulting in short-chain carboxylic acids that eventually mineralize to CO_2 (Beqqal et al. 2017, Arhoutane et al. 2019).

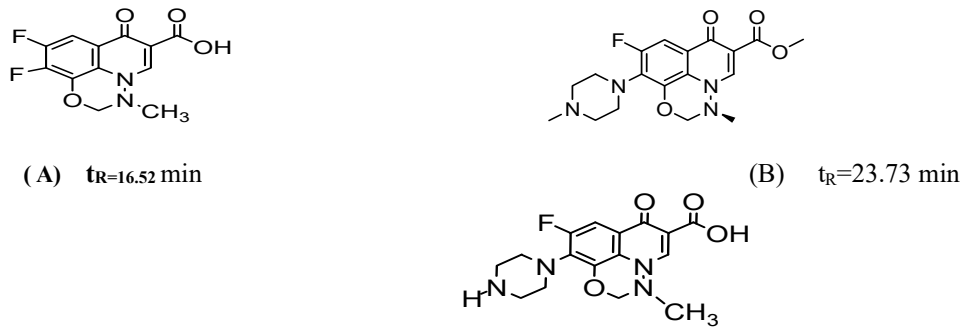

(A) $t_{R=16.52}$ min (B) t_R=23.73 min

(C) $t_{R=21.95}$ min

Fig. 8. HPLC was used to identify intermediates after electro-Fenton treatment and compare their retention durations to those of Marbo degradation in genuine samples

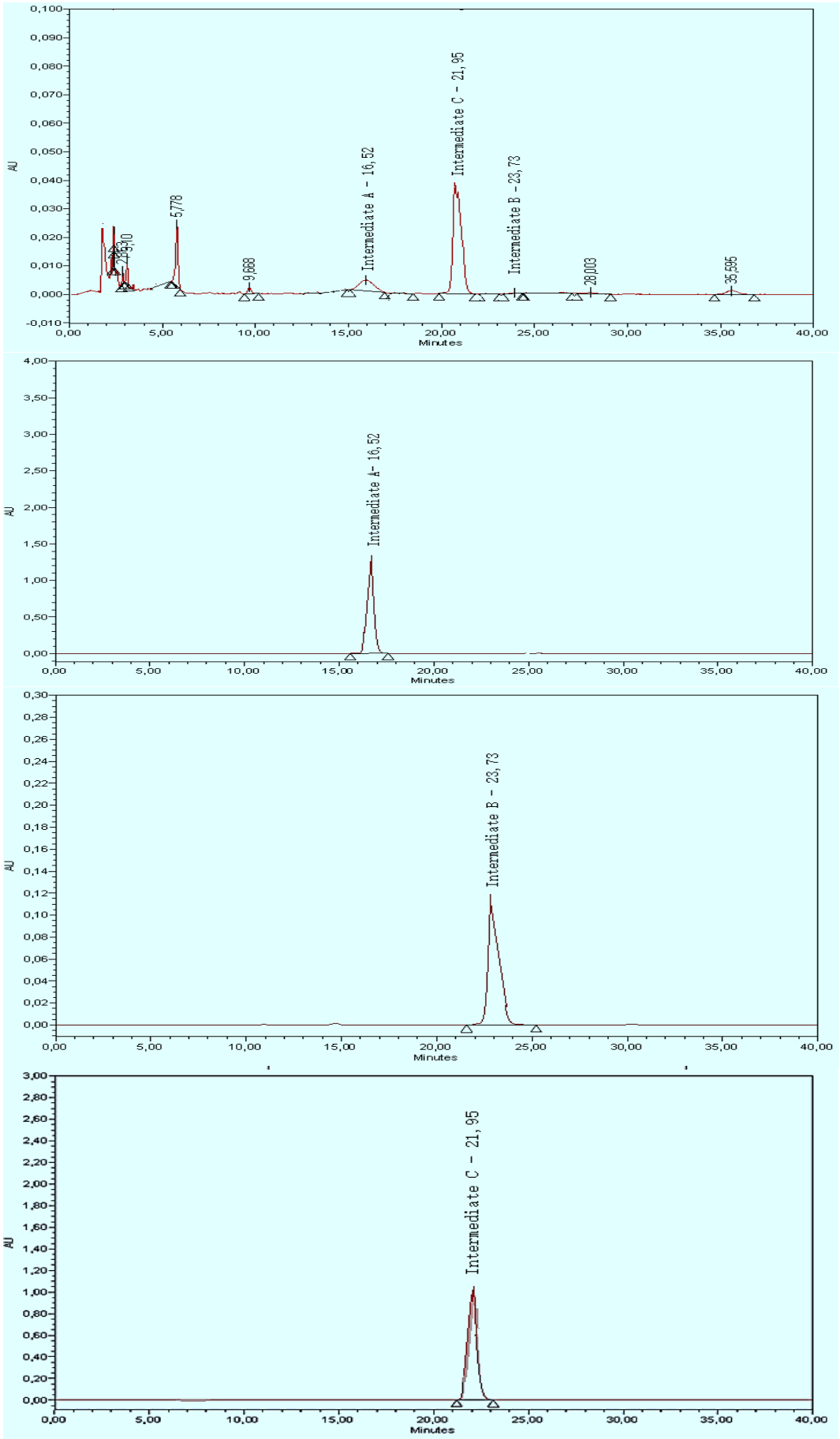

Fig. 9. HPLC Chromatogram Displaying the Electro-Fenton Degradation of Marbofloxacin (0.144 mM) Over an (11) Minute Period. Conditions: Applied Current of 100 mA, Fe^{2+} Concentration of 0.1 mM, [Na_2SO_4] at 50 mM, Volume of 200 mL, and pH = 3

Analyzing inorganic ion release into the solution throughout the treatment protocol provides additional corroborative evidence supporting the mineralization process. The organic contaminant in question, characterized by its intricate molecular architecture, presents substantial challenges to degradation mechanisms (Brillas et al. 2009, Yahya et al. 2023, Arhoutane et al. 2019). Nevertheless, mineralization facilitated the effective conversion of these organic compounds into inorganic ions. Upon attaining an elevated oxidation state, the solution demonstrated the emergence of liberated NH_4^+, NO_3^-, and fluoride ions. Noteworthy is the observation that the fluoride ion concentration reached a zenith of 0.14 mM, while nitrogen entities, largely deriving from the original Marbo pollutant, were predominantly transformed into NH_4^+ ions. At the termination of the mineralization sequence (360 minutes), the aggregate concentration of NH_4^+ and NO_3^- ions amounted to 0.406 mM, constituting approximately 90% of the initial nitrogen quota. These outcomes robustly substantiate the successful mineralization of Marbo, as graphically illustrated in Fig. (10) (Yanga et al. 2023, Yahya et al. 2015).

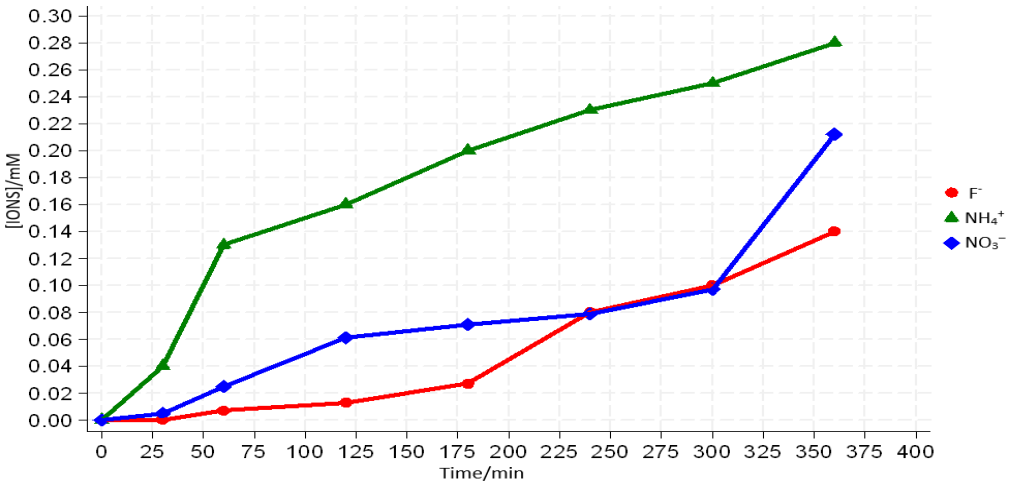

Fig. 10. Evolution of Inorganic Ions During the Electro-Fenton Process Using CF/Pt Electrodes. Experimental Setup: Initial Marbofloxacin Concentration of 0.144 mM, Fe^{2+} at 0.1 mM, [Na_2SO_4] at 50 mM, Volume of 200 mL, pH 3, and Ambient Temperature

The biodegradation and mineralization of the Marbo molecule were investigated under electrolysis conditions at a current intensity of 300 mA using Fe^{2+} (0.10 mM) as a catalyst. The initial absence of a BOD_5/COD ratio indicated the non-biodegradability of the Marbo molecule. However, following 3 hours of electrolysis, a notable increase in biodegradability was observed, as evidenced by a BOD_5/COD ratio of 1.403, suggesting the generation of intermediate degradation products (Yu, Y et al. 2018). Further electrolysis for a longer period significantly enhanced biodegradability, with a BOD_5/COD ratio of 6.34 (Fig. 11).

The synergistic integration of electro-Fenton catalysis with subsequent biological post-treatment emerges as a promising strategy for the tailored optimization of electrolysis duration in the degradation of Marbo pharmaceutical compounds. This innovative approach aims to enhance biodegradability while facilitating a seamless transition to biological remediation, thereby offering a cost-effective and environmentally sustainable solution.

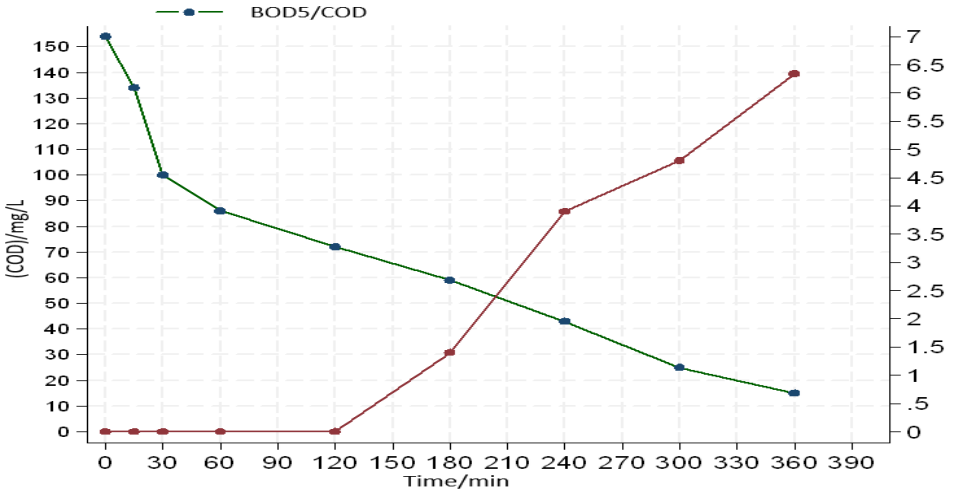

Fig. 11. Assessment of the advancement of biodegradation and chemical oxygen demand (COD) mineralization during Electro-Fenton for [Marbo]= 0.144 mM, Fe^{2+} at 0.1 mM, [Na_2SO_4] at 50 mM, Volume of 200 mL, pH 3, and Ambient Temperature

Strengths and Limitations

This study stands out due to its rigorous application of statistical analyses, which effectively delineate the complex dynamics that govern the electro-Fenton degradation process. This has provided a comprehensive understanding of how various operational parameters interact and influence degradation efficiency, offering a robust foundation for optimizing treatment conditions. Furthermore, the investigation into releasing inorganic ions as evidence of mineralization significantly contributes to the field by offering clear and quantifiable measures of the process's success.

However, it is important to acknowledge the limitations of this study. While valuable insights have been gained regarding the electro-Fenton process, the exclusive focus on marbofloxacin as the sole pollutant of interest may limit the generalizability of the findings to other contaminants. Additionally, exploring side reactions, particularly at higher current densities, necessitates further investigation to understand their impact on treatment efficiency and energy consumption fully.

Implications for Practice and Research

For environmental engineering practice, this study highlights the critical importance of selecting appropriate cathode materials and operational parameters to enhance the efficiency of the electro-Fenton process in water treatment applications. The insights gained here should guide the development of more effective and energy-efficient treatment strategies for pharmaceutical contaminants, with the potential to extend to a wider range of organic pollutants.

In terms of research implications, this work paves the way for future studies to expand the scope of pollutants treated through the electro-Fenton process, explore alternative cathode materials, and further optimize operational parameters for increased efficiency. Investigating the mechanisms underlying the observed side reactions and their impact on treatment outcomes will also be crucial for advancing the field.

In conclusion, this study contributes significantly to the knowledge of electro-Fenton processes, offering practical insights for environmental protection and public health through improved water treatment technologies.

5. Conclusion

This comprehensive study has systematically explored the efficacy of the electro-Fenton process in degrading and mineralizing marbofloxacin, a pharmaceutical contaminant of significant environmental concern. Through meticulous experimentation and robust statistical modeling, we have illuminated the complex interactions between operational parameters—namely, cathode material, current density, and Fe^{2+} catalyst concentration – and their collective impact on the treatment process. Our findings underscore the electro-Fenton process's potential as an environmentally friendly and effective method for remediating water contaminated with complex organic pollutants.

The comparative analysis conducted on carbon felt (CF) and graphite carbon (CG) cathodes under various operational conditions revealed that CF cathodes, especially at an optimal current density of 300 mA, demonstrate superior performance in terms of marbofloxacin degradation and COD removal efficiency. This

highlights the significance of selecting the appropriate cathode material and calibrating the current density to maximize the effectiveness of the electro-Fenton process. Moreover, the study has established that lower concentrations of the Fe^{2+} catalyst (0.05 mM and 0.1 mM) are unexpectedly more effective, pointing towards an optimal catalytic interplay that enhances marbofloxacin's electrochemical degradation and enhances their biodegradability.

Statements and Declarations

Disclosure statement

No potential conflict of interest was reported by the author(s).

Ethics approval statement

This is an observational study for which no ethical approval is required.

Data availability

Data generated or analyzed during this study are provided in full within the published article.

Informed consent statement

Samples of human beings or animals were not used for this study; hence, no consent statement is needed.

Additional information

Funding

No funding was obtained for this study.

Competing interests

The authors declare no competing financial interest.

References

Arhoutane, M.R., Yahya, M.S., El Karbane, M., Guessous, A., Chakchak, H., El Kacemi, K. (2019). Removal of pyrazinamide and its by-products from water: Treatment by electro-Fenton process and feasibility of a biological post-treatment. *Mediterranean Journal of Chemistry*, *8*(1), 53-65. http://dx.doi.org/10.13171/mjc811903420mra

Arhoutane, M.R., Yahya, M.Sh., El Karbane, M., El Kacemi, Kacem. (2019). Oxidative degradation of gentamicin present in water by an electro-Fenton process and biodegradability improvement. *Open Chem*., *17*, 1017-1025. doi.org/10.1515/chem-2019-0110

Beqqal, N., Yahya, M.S., Karbane, M., Guessous, A., El Kacemi, K. (2017). Kinetic study of the degradation/mineralization of aqueous solutions contaminated with Rosuvastatin drug by Electro-Fenton: Influence of experimental parameters. *Journal of Materials and Environmental Sciences*, *8*(12), 4399-4407.

Brillas, E., Sirés, I., Oturan, M.A.(2009). Electro-Fenton process and related electrochemical technologies based on Fenton's reaction chemistry. *Chemical reviews, 109*(12), 6570-6631. https://doi.org/10.1021/cr900136g

Ganiyu, S.O., Martínez-Huitle, C.A., Oturan, M.A. (2021). Electrochemical advanced oxidation processes for wastewater treatment: Advances in formation and detection of reactive species and mechanisms. *Current Opinion in Electrochemistry*, *27*, 100678. http://dx.doi.org/10.1016/j.coelec.2020.100678

Garcia-Segura, S., Mostafa, E., Baltruschat, H. (2017). Could NO_x be released during mineralization of pollutants containing nitrogen by hydroxyl radical? Ascertaining the release of N-volatile species, Applied Catalysis B: *Environmental*, *207*, 376-384.

Haji, I., Shueai Yahya, M., Rachidi, L., Warad, I., Zarrouk, A.M., Talidi, A., El Karbane, M., Kaichouh, G. (2024). Bio-Electro-Fenton Process: Application to the Antiviral Ribavirin Mineralization in Aqueous Medium. *Analytical and Bioanalytical Electrochemistry*, *16*(1), 79-99. https://www.doi.org/10.22034/abec.2024.710596

Lahkimi, A., Oturan, M. A., Oturan, N., Chaouch, M. (2007). Removal of Textile Dyes From Water by the Electro-Fenton Process. *Environmental Chemistry Letters*, *5*, 35-39. http://dx.doi.org/10.1007/s10311-006-0058-x

Nidheesh, P., Gandhimathi, R. (2012). Trends in electro-Fenton process for water and wastewater treatment: An overview, An Overview. *Desalination*, *299*, 1-15. https://doi.org/10.1016/j.desal.2012.05.011

Nidheesh, P., Gandhimathi, R., Sanjini, S. (2014). $NaHCO_3$ enhanced Rhodamine B removal from aqueous solution by graphite–graphite electro Fenton system. *Separation and Purification Technology*, *132*, 568-576. http://dx.doi.org/10.1016/j.seppur.2014.06.009

Oturan, M.A., Oturan, N., Lahitte, C., Trévin, S. (2001). Degradation of three pesticides used in viticulture by electro-generated Fenton's reagent. *J. Electroanal. Chem*., *507*, 96-102. https://doi.org/10.1051/agro:2005005

Oturan, N.,Oturan, M.A. (2018). Chapter 8 – Electro-Fenton Process: Background, New Developments, and Applications. *Electrochemical Water and Wastewater Treatment*, Elsevier, 193-221. http://dx.doi.org/10.1016/B978-0-12-813160-2.00008-0

Özcan, A., Şahin, Y., Koparal, A.S., Oturan, M.A. (2008). Carbon Sponge as a New Cathode Material for the Electro-Fenton Process: Comparison with Carbon Felt Cathode and Application to Degradation of Synthetic Dye Basic Blue 3 in Aqueous Medium. *Journal of Electroanalytical Chemistry*, *616*(1-2), 71-78. http://dx.doi.org/10.1016/j.jelechem.2008.01.002

Qiang, Z., Chang, J-H., Huang, C.-P. (2002). Electrochemical generation of hydrogen peroxide from dissolved oxygen in acidic solutions. *Water Research*, *36*(1), 85-94. https://doi.org/10.1016/s0043-1354(01)00235-4

Rabab A, Hakami., Afnan A, Hakami., Muna Shueai, Yahya. (2024). Effect of the Cathode Material on the Efficiency of the Electro-Fenton Process to Remove Pefloxacin. Kinetics And Oxidation Products. *Environment Protection Engineering*, *2*(50). https://doi.org/10.37190/epe240205

Rabab A, Hakami., Muna Shueai, Yahya., Afnan A, Hakami., Ghizlan, Kaichouh., Mohamed, El Bakkali. (2024). Grepafloxacin degradation and mineralization in water by Electro-Fenton process. *International Journal of Electrochemical Science*, *19*, 100556. https://doi.org/10.1016/j.ijoes.2024.100556

Sirés, I., Brillas, E., Oturan, M.A., Rodrigo, M.A., Panizza, M. (2014). Electrochemical advanced oxidation processes: today and tomorrow. A review, *Environmental Science and Pollution Research*, *21*, 8336-8367. https://doi.org/10.1007/s11356-014-2783-1

Sopaj, F., Oturan, N., Pinson, J., Podvorica, F., Oturan, M.A. (2016). Effect of the anode materials on the efficiency of the electro-Fenton process for the mineralization of the antibiotic sulfamethazine. *Applied Catalysis B: Environmental*, *199*, 331-341.

Sturini, M., Speltini, A., Maraschi, F., Rivagli, E., Pretali, L., Malavasi, L., Profumo, A., Fasani, E., Albini, A. (2015). Sunlight photodegradation of marbofloxacin and enrofloxacin adsorbed on clay minerals. *Journal of Photochemistry and Photobiology A: Chemistry*, *299*, 103-109. https://doi.org/10.1016/j.jphotochem.2014.11.015

Yahya, M.S., Beqqual, N., Haji, I., Karbane, M.E., Chakchak, H., Warad, I., Zarrouk, A.M., Kaichouh, G. (2023). Optimization of the Electro-Fenton Process for the Elimination of Oxytetracycline Antibiotic from Water: Degradation/Mineralization Kinetics. *Analytical and Bioanalytical Electrochemistry*, *15*(4), 251-263. https://www.doi.org/10.22034/abec.2024.710596

Yahya, M.S., El Karbane, M., Oturan, N., El Kacemi, K., Oturan, M.A. (2015). Mineralization of the antibiotic levofloxacin in aqueous medium by electro-Fenton process: Kinetics and intermediate products analysis. *Environmental technology*, *37*(10), 1276-1287. http://dx.doi.org/10.1080/09593330.2015.1111427

Yahya, M.S., Oturan, N., El Kacemi, K., El Karbane, M., Aravindakumar, C., Oturan, M.A. (2014). Oxidative degradation study on antimicrobial agent ciprofloxacin by electro-fenton process: Kinetics and oxidation products. *Chemosphere*, 117, 447-454. http://dx.doi.org/10.1016/j.chemosphere.2014.08.016

Yang, W.L, Oturan, N., Raffy, S., Zhou, M.H., Oturan, M.A. (2020). Electrocatalytic generation of homogeneous and heterogeneous hydroxyl radicals for cold mineralization of anticancer drug Imatinib. *Chemical Engineering Journal*, *383*, 123155. https://doi.org/10.1016/j.cej.2019.123155

Yanga, W., Oturan, N., Lianga, J., Oturan, M. (2023). Synergistic mineralization of ofloxacin in electro-Fenton process with BDD anode: Reactivity and mechanism. *Separation and Purification Technology*, *319*, 124039. https://doi.org/10.1016/j.seppur.2023.124039

Yu, Y., Huang, F., He, Y., Liu, X., Song, C., Xu, Y., Zhang, Y. (2018). Heterogeneous fenton-like degradation of ofloxacin over sludge derived carbon as catalysts: Mechanism and performance. *Sci. Total Environ*, *654*, 942-947. https://doi.org/10.1016/j.scitotenv.2018.11.156

Zazou, H., Oturan, N., Çelebi. M.S., Hamdani, M., Oturan, M.A. (2019). Cold incineration of 1, 2-dichlorobenzene in aqueous solution by electrochemical advanced oxidation using DSA/Carbon felt, Pt/Carbon felt and BDD/Carbon felt cells. *Separation and Purification Technology*, *208*, 184-193. https://doi.org/10.1016/j.seppur.2018.03.030